ПЛОВДИВСКИ УНИВЕРСИТЕТ "ПАИСИЙ ХИЛЕНДАРСКИ", БЪЛГАРИЯ
НАУЧНИ ТРУДОВЕ, ТОМ 35, КН. 3, 2007 – МАТЕМАТИКА
PLOVDIV UNIVERSITY "PAISSII HILENDARSKI", BULGARIA
SCIENTIFIC WORKS, VOL. 35, BOOK 3, 2007 – MATHEMATICS

NUMERICAL SIMULATION OF BIFURCATIONAL CURVES IN LONG NON-HOMOGENEOUS JOSEPHSON JUNCTIONS

P. Kh. Atanasova, T. L. Bojadjiev

Abstract. The bifurcations of the solutions of multiparametric nonlinear boundary problem in Physics of Josephson junctions (JJ) are investigated numerically. Two cases are considered: JJ with overlap geometry and with in-line geometry. In order to study the stability of the solution of the nonlinear boundary problem with respect to small "space-time" perturbations a Sturm-Liouville problem generated from this solution is considered. The bifurcational points are calculated by the continuous analogue of the method of Newton. A good coincidence of the numerical results and experimental data is received. Some numerical results and an investigation of the critical curves are illustrated graphically.

Key words: numerical simulation, long non-homogeneous junction, overlap geometry, in-line geometry, Josephson, Sturm-Liouville, sine-Gordon, bifurcational curves, continuous analogue of the method of Newton, soliton, fluxon

Mathematics Subject Classification 2000: 33F05, 34B15, 34B24, 34K28, 34L16, 74K30

1. Statement of the problem

In this paper the bifurcations of the solutions of multiparametric nonlinear boundary problems in Physics of Josephson junctions (JJ) are investigated numerically.

The basic physical quantity which characterizes JJ is a phase difference $\varphi(x)$ of the wave functions of both superconductors. At a suitable normalization the phase difference can be considered as a magnetic flux across the junction.

The junctions is one-dimensional (or long) if one of the dimensions (for instance x) is much more longer than the two other dimensions (y and z).

The stationary (independent on the time) distributions of the magnetic flux $\varphi(x)$ satisfy a nonlinear differential equation of second order so called perturbed sine-Gordon equation. The exact form of the equation for the magnetic flux depends on the physical conditions at which JJ is considered. The following two cases are most popular in practice.

A. JJ with overlap geometry. In this case the external current flows along the x-axis during the entire junction ($x \in [-\Delta, \Delta]$, where Δ is the half-length of the JJ) and it can be considered approximately as a constant. Some more precise models taking into account the change of the current γ along the length of JJ and the connected with this physical effects are considered in the papers [22, 23].

In the case of JJ with overlap geometry the sine-Gordon equation for the magnetic flux $\varphi(x)$ has the following form

$$-\varphi_{xx} + j_D(x)\sin\varphi + \gamma = 0, \tag{1.1}$$

and the boundary conditions are "symmetric" conditions of Neuman type.

$$\varphi_x(-\Delta) = h_B, \quad \varphi_x(\Delta) = h_B. \tag{1.2}$$

In the expressions shown above the function $j_D(x)$ is a given function of independent variable x describing the amplitude of Josephson critical current and the magnitude h_B is a constant which from the physical point of view expresses the voltage of a magnetic field at the ends of JJ.

Let us note that here and further in the paper the physical magnitudes are dimensionless. The method for reducing of equations into the dimensionless form is described in [2].

B. JJ with "in-line" geometry. In this case the current γ flows "only" at the ends of JJ. The magnetic flux $\varphi(x)$ satisfies the nonlinear ordinary differential equation

$$-\varphi_{xx} + j_D(x)\sin\varphi = 0, \tag{1.3}$$

with "non-symmetric" boundary conditions of the kind

$$\varphi_x(-\Delta) = h_L \equiv h_B - \alpha_L\gamma, \quad \varphi_x(\Delta) = h_R \equiv h_B - \alpha_R\gamma. \tag{1.4}$$

Here α_L and α_R are parameters satisfying the condition $\alpha_L + \alpha_R = 1$.

Further we shall consider in details the case of JJ with "in-line" geometry comparing our results with the known ones for JJ with overlap geometry.

In order to study the stability of the solution $\varphi(x)$ of the nonlinear boundary problem (1.3), (1.4) with respect to small "space-time" perturbations we consider the generated from this solution differential Sturm-Liouville problem (SLP)

$$-\psi_{xx} + q(x)\psi = \lambda\psi, \tag{1.5}$$

$$\psi_x(-\Delta) = 0, \quad \psi_x(\Delta) = 0, \tag{1.6}$$

with a potential $q(x) = j_D(x)\cos\varphi(x)$. Evidently in this case we have $-1 \le q(x) \le 1$.

It is well-known [18] that SLP (1.5), (1.6) in this case has infinite number of bounded below eigen-values (EV)

$$\lambda_{\min} = \lambda_0 < \lambda_1 < \cdots < \lambda_n < \cdots$$

and to every EV λ_n corresponds one and only one eigen-function (EF) $\psi_n(x)$ satisfying the normalizing condition

$$\langle\psi,\psi\rangle \equiv \int_{-\Delta}^{\Delta} \psi_n^2(x)dx = 1. \tag{1.7}$$

According to the theorem of oscillations [18] the number of zeros of EF $\psi_n(x)$ in the interval $[-\Delta,\Delta]$ equals the index n.

PSL gives a simple stability criterion [2]. If the solution $\varphi(x)$ is stable then the corresponding to this solution minimal EV $\lambda_{\min}$ is positive. If the solution $\varphi(x)$ is unstable — $\lambda_{\min}$ is negative. The case $\lambda_{\min} = 0$ corresponds to the stability station switches to unstability one or vice versa. This method is justified in the work [2] and developed in the papers [4, 15–17]. We shall note that every solution $\varphi(x)$ of (1.3), (1.4) depends not only on the coordinate x but on the physical parameters h_B and γ, as well. Then the potential $q(x)$ and therefore EV λ_n and EF $\psi_n(x)$ of SLP will also depend on the magnitudes h_B and γ. The dependence expressed by the equation

$$\lambda_{\min}(h_B,\gamma) = 0, \tag{1.8}$$

defines geometrically a curve in the plane (h_B,γ). This curve is called a bifurcational curve (BC) for the given solution. Let us note that in contrast to EV and EF the envelope of BCs can be obtained experimentally. Sometimes in the physical literature the term "a critical curve" is used.

We suppose that the dielectric layer in JJ is, in general, non-homogeneous. Physically this means that the thickness (the size in z-axes) of the dielectric layer (see fig. 1a) can change along the length x of JJ. The non-homogeneity is simulated by the function $j_D(x) \in [0, 1]$. Evidently in a homogeneous junction $j_D(x) = 1$.

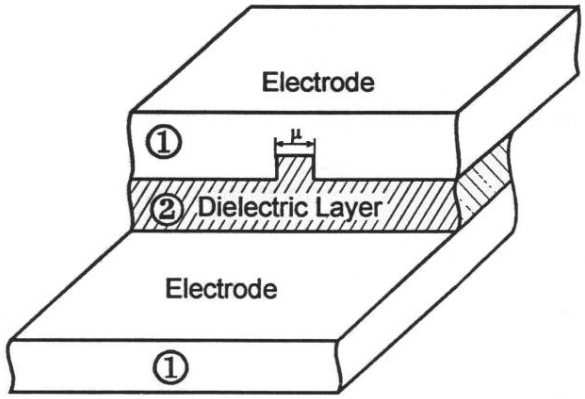

Fig. 1a

Further, we shall consider the case of a junction which dielectric layer has only one non-homogeneity of resistable type which is disposed in the center of the junction.

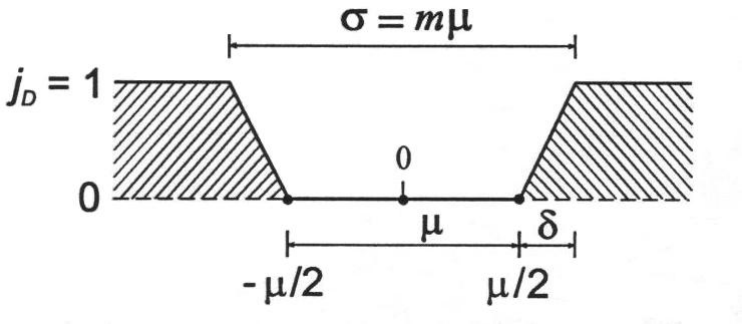

Fig. 1b

The real non-homogeneities of JJ have limited sizes which must be taken into account in the numerical simulations. That is why in this work the amplitude of the current $j_D(x)$ in JJ is modelled by a trapezoid (fig 1b) with a base μ and a height 1. The upper base has a length $\sigma = m\mu$, where $m \geq 1$ is a parameter depending on the technology of preparation of the corresponding pattern. At $m = 1$ the non-homogeneity is a rectangle with a base equal to μ. The change of the current from 0 to 1 in such a non-homogeneity passes in the interval $\delta = (m-1)\mu/2$ which is determined by the corresponding width μ. All the numerical calculations in the presented work are done at $\mu = 1.5$.

The analytical expression for the amplitude $j_D(x)$ in a junction with one non-homogeneity with a center in the point $x = 0$ has a form $j_D = 1-\zeta(x, \mu, m)$ where

$$\zeta(x) = \frac{2m}{\mu(1+m)}\Big[(x+\frac{\mu}{2m})_+ - (x+\frac{\mu}{2})_+ - (x-\frac{\mu}{2})_+ + (x-\frac{\mu}{2m})_+\Big]$$

and x_+ denotes the unit step-function of Heavyside.

Let us note that in the case of rectangular non-homogeneity ($m = 1$) the boundary problem (1.3), (1.4) is written in details as follows

$$\varphi_x(-\Delta) = h_B - \alpha_L\gamma; \tag{1.9}$$

$$-\varphi_{xx} + \sin\varphi = 0, \quad \text{for } x \in (-\Delta, \mu/2); \tag{1.10}$$

$$\varphi(-\mu/2-0) - \varphi(-\mu/2+0) = 0; \tag{1.11}$$

$$\varphi_x(-\mu/2-0) - \varphi_x(-\mu/2+0) = 0; \tag{1.12}$$

$$-\varphi_{xx} = 0, \quad \text{for } x \in (-\mu/2, \mu/2); \tag{1.13}$$

$$\varphi(\mu/2-0) - \varphi(\mu/2+0) = 0; \tag{1.14}$$

$$\varphi_x(\mu/2-0) - \varphi_x(\mu/2+0) = 0; \tag{1.15}$$

$$-\varphi_{xx} + \sin\varphi = 0, \quad \text{for } x \in (\mu/2, \Delta); \tag{1.16}$$

$$\varphi_x(\Delta) = h_B - \alpha_R\gamma; \tag{1.17}$$

At given values of the parameters the problem (1.9)–(1.17) allows a formal analytic solution which can be written in quadratures by elliptic functions. Actually, the equations (1.10) and (1.16) allow the first integrals (of the "energy")

$$\frac{\varphi_x^2}{4} = k_j - \cos^2\frac{\varphi}{2},\ j = 1, 2\ , \tag{1.18}$$

where k_j are the integration constants. It follows from here that outside of the non-homogeneity i.e. when $x \in [-\Delta, -\mu/2) \cup (\mu/2, \Delta]$ the general solution has the form

$$\cos\frac{\varphi}{2} = -k_j \mathrm{sn}(x + \ell_j, k_j), \tag{1.19}$$

where $\mathrm{sn}(x, k)$ is the elliptic sine of Jacoby and ℓ_j are the integration constants.

When $x \in (-\mu/2, \mu/2)$ i.e. inside the non-homogeneity the general solution is a linear function

$$\varphi(x) = a_1 x + a_2 \tag{1.20}$$

with parameters $a_j, j = 1, 2$.

In this way, in the equations (1.19) and (1.20) enter 6 arbitrary constants $k_j,\ a_j,\ \ell_j,\ i = 1, 2$. In order to calculate all of them we have a closed system of equations from the conditions (1.9), (1.11), (1.12), (1.14), (1.15) and (1.17). If the junction is homogeneous then the number of the integration constants is 4.

An analysis of the upper scheme in the case of a homogeneous or non-homogeneous JJ with Dirac δ-shaped non-homogeneities is presented in the works [2,19,14]. The solving of the algebraic system for the parameters (integration constants) in the case of a non-homogeneous JJ with a rectangular non-homogeneity is connected with considerable technical difficulties. This method leads to more serious difficulties in the construction of the BCs. This is the reason that in the present work the direct numerical modeling of the system (1.3)–(1.7) is prefered.

Using the algorithm originally described in the paper [15] BCs (critical curves) for the solutions in JJ with a single non-homogeneity corresponding to different values of the width μ of the non-homogeneity are constructed. It is shown that the envelope of BCs for a given μ of the form "current-magnetic field" $\lambda_{\min}(h_B, \gamma) = 0$ has singularities which do not exist in homogeneous JJ. Namely, the local maximums of the critical (maximal) current γ at fixed values of the magnetic field h_B, and also "zones of damping" (intervals for h_B in which the maximal current is zero) do not exist. This phenomenon is

marked for the first time in the work [6] for the case of Josephson lattices which dielectric layer consists of a big number of periodically distributed non-homogeneities. An attempt of theoretical analysis of this phenomenon using mechanical analogues is made in the paper [21].

Our numerical results prove that the pointed out phenomenon appears because of the presence of the non-homogeneity and depends on the kind of the boundary conditions and it is not connected with a periodicity (lattice).

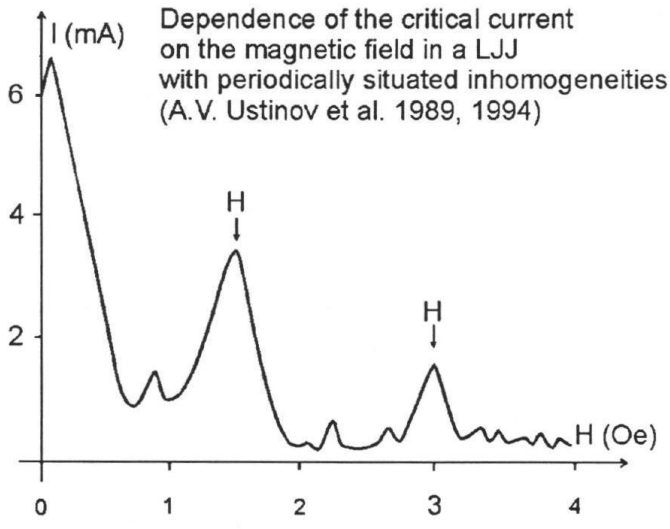

Fig. 2

It should also be noted that the known in the physical experimental data [5–7] contain a very important from the physical point of view but not sufficiently discussed by the authors peculiarity consisting of displacement (see fig.2) of the central maximum (corresponding to so called "Meissner" solution as we shall show bellow) of the critical curve of the kind "current-magnetic field" $\lambda_{\min}(h_B, \gamma) = 0$ from the point $h_B = 0$. Our numerical results show that the analogous displacement arises as a result of the non-homogeneity of the boundary conditions. From the physical point of view this means that the marked effect is actually a consequence of the conditions of the experiment (current injection through the ends of JJ).

2. Continuous analogue of the method of Newton

In the present work for the formulated above bifurcational problem we shall use the continuous analogue of the method of Newton (CAMN). We shall explain the main idea of CAMN on the base of single nonlinear equation of the form

$$f(x) = 0 \tag{2.1}$$

where $f(x)$ is a given function with a necessary smoothnees. We suppose that the equation (2.1) has a real root x^*. In the classic method of Newton [10] an approximate solution of (2.1) is finding by the iterational process

$$f'(x^n).w^n = -f(x^n), \quad n = 0, 1, 2, \dots \ . \tag{2.2}$$

The problem (2.2) is a linear equation with respect to w^n and x^0 is a given initial approximation. The next approximation to the exact solution is determined by the formula

$$x^{n+1} = x^n + w^n. \tag{2.3}$$

The convergence of the iterational process (2.2) in the neighbourhood of an exact solution x^* is quadratic [10]. If the choice of the initial approximation x^0 is not suitable then the process (2.2) turns out to be divergent.

The basic idea of CAMN (see the original work of Gavurin [8] and the survey [9] as well) consists of the presentation of the "motion" between the points x^0 and x^* by the curve $x(t)$ depending on the continuous parameter t (an analogue of the time). "The trajectory" $x(t)$ satisfies the ordinary differential equation (Gavurin's equation)

$$f'(x).\dot{x} = -f(x) \tag{2.4}$$

which "obviously" has the first integral $f(x) = f(x^0).e^{-t}$. If the magnitude $f(x^{(0)})$ is bounded then from the last equality it follows the convergence of the "path" $x(t)$ at $t \to \infty$ to the exact solution x^*. From here one of the principal advantages of CAMN is seen. This is the possibility for a considerable extension of the convergence region.

In the numerical realization of CAMN several discretizations of Gavurin's equation (2.4) can be used. The most simple and at the same time sufficiently effective is the Euler's scheme [9]. In this case the "time" t is replaced by the discrete parameter $\tau_n = t_{n+1} - t_n$ and the derivative $w = \dot{x}$ is replaced by the difference analogue $w^n = (x^{n+1} - x^n)/\tau_n$. Thus at each iteration n (at every

"layer" t_n) we reach the equation (2.2) again, but now the next approximation x^{n+1} depends on the step τ_n and we calculate it by the formula

$$x^{n+1} = x^n + \tau_n w^n \ . \tag{2.5}$$

It is clear that at $\tau_n = 1$ the iterations are those which are derived from the classic method of Newton.

The quantity τ_n is usually determined by the condition of minimum of the error

$$\delta(\tau_n) = f^2(x^n + \tau_n w^n) \tag{2.6}$$

which ensures the best convergence. For this purpose a series of methods are developed. In our point of view the most algorithmically simple is the method of Ermakov and Kalitkin [11]. The basic idea of this method consists of approximate presentation of the dependence (2.6) in the interval $\delta(\tau_n) \in (0, 1)$ by a parabola and the point τ_{opt} of the minimum of this parabola gives us the "optimal" value of the step

$$\tau_{\text{opt}} = \delta(0)/(\delta(0) + \delta(1)). \tag{2.7}$$

Here $\delta(0)$ is the discrepancy of a current approximation x^n, and $\delta(1)$ is the discrepancy of the approximation obtained from x^n by the pure newtonian step ($\tau_n = 1$).

3. Application of CAMN for calculation of bifurcational points

We apply the development of CAMN for the solving of the formulated in §1 problem of calculation of bifurcation curves (1.3)–(1.7). For this purpose, we consider these equations at fixed length 2Δ, width μ of the junction and parameters α_L and α_R, as an united system for the unknown functions $\varphi(x)$ and $\psi(x)$ in which the three parameters h_B, γ and λ take place. In order that the system be closed we must set the two of these parameters and then the third of them can be considered as EV of a nonlinear spectral problem. In the "trivial" case we set the magnitudes h_B and γ. Then the system decomposes itself into two independently subsystems for the variable $\varphi(x)$ and $(\psi(x), \lambda)$, which denotes that we verify the stability of the solution $\varphi(x)$. The spectral parameter in this case is the magnitude λ. In the other two cases (γ and λ, or h_B and λ given) the system must be considered as a nonlinear EV problem with a spectral parameter h_B and γ respectively.

Further, we consider the case in which h_B is chosen as a spectral parameter.

Let us fix the parameters γ and λ and let us consider the function

$$f(z) = \begin{cases} -\varphi_{xx} + j_D(x)\sin\varphi \\ \varphi_x(-\Delta) - h_L \\ \varphi_x(\Delta) - h_R \\ -\psi_{xx} + [j_D(x)\cos\varphi - \lambda]\psi \\ \psi_x(-\Delta) \\ \psi_x(\Delta) \\ \langle\psi,\psi\rangle - 1 \end{cases},$$

where for the sake of simplicity (φ, ψ, h_B) is set by z. We suppose that the equation

$$f(z) = 0 \tag{3.1}$$

has an isolated solution z^* i.e. there exists a neighbourhood $|z - z^*| < \varepsilon$ in which the condition $f(z) \neq 0$ is fulfilled. Then the equation (2.2) will take the form

$$-u_{xx} + q(x)u = \varphi_{xx} - j_D(x)\sin\varphi, \tag{3.2}$$

$$u_x(-\Delta) - p = h_L - \varphi_x(-\Delta), \quad u_x(\Delta) - p = h_R - \varphi_x(\Delta), \tag{3.3}$$

$$-v_{xx} + [q(x) - \lambda]v + j_D(x)\sin\varphi u\psi = \psi_{xx} - [q(x) - \lambda]\psi, \tag{3.4}$$

$$v_x(-\Delta) = -\psi_x(-\Delta), \quad v_x(\Delta) = -\psi_x(\Delta), \tag{3.5}$$

$$2\langle\psi, v\rangle = 1 - \langle\psi,\psi\rangle, \tag{3.6}$$

where $\{\dot{\varphi}, \dot{\psi}, \dot{h}_B\} \equiv \{u(x), v(x), p\}$ is denoted by w and we have

$$\dot{\varphi} = u, \quad \dot{\psi} = v, \quad \dot{h}_B = p. \tag{3.7}$$

For the sake of brevity in (3.2)–(3.7) the iteration number n is omited. In order to decompose the system (3.2)–(3.6) we shall look for the solution in the form of a linear combination

$$u(x) = u_1(x) + pu_2(x), \quad v(x) = v_1(x) + pv_2(x), \tag{3.8}$$

where u_1, u_2, v_1, v_2 are new unknown functions of the independent variable x, and p is a parameter (the derivative of the magnetic field h_B with respect to the "time"). If we substitute the correlations (3.8) into (3.2)–(3.6) and if the coefficients in front of the derivative p are set to be zero then we receive

$$-u_{1,xx} + q(x)u_1 = \varphi_{xx} - j_D(x)\sin\varphi, \tag{3.9}$$

$$u_{1,x}(-\Delta) = h_L - \varphi_x(-\Delta), \quad u_{1,x}(\Delta) = h_R - \varphi_x(\Delta), \tag{3.10}$$

$$-u_{2,xx} + q(x)u_2 = 0, \tag{3.11}$$

$$u_{2,x}(-\Delta) = 1, \quad u_{2,x}(\Delta) = 1, \tag{3.12}$$

$$-v_{1,xx} + [q(x) - \lambda]v_1 = \psi_{xx} - [q(x) - \lambda]\psi - j_D(x)\sin\varphi\psi u_1, \tag{3.13}$$

$$v_{1,}x(-\Delta) = -\psi(-\Delta), \quad v_{1,x}(\Delta) = -\psi(\Delta), \tag{3.14}$$

$$-v_{2,xx} + [q(x) - \lambda]v_2 = -j_D(x)\sin\varphi\psi u_2, \tag{3.15}$$

$$v_{2,x}(-\Delta) = 0, \quad v_{2,x}(\Delta) = 0. \tag{3.16}$$

The obtained expressions allow to define the following algorithm for the calculation of the bifurcation points along the parameter h_B of the solutions in JJ:

A. For a given solution $\varphi(x)$, $\psi(x)$ and h_B at n-th iteration, we calculate the functions $u_1(x)$ and $u_2(x)$ from the linear boundary problem (3.9)–(3.12).

B. We replace the known magnitudes in (3.13)–(3.16). We find the left sides of the last system and calculate the corresponding solutions $v_1(x)$ and $v_2(x)$.

C. At known $v_1(x)$ and $v_2(x)$ we calculate the increase p of the bifurcation parameter h_B of a current iteration from the equation

$$p = \frac{1 - \langle\psi,\psi\rangle - 2\langle v_1,\psi\rangle}{2\langle v_2,\psi\rangle}, \tag{3.17}$$

which follows from (3.6).

D. The next approximation for $\varphi(x)$, $\psi(x)$ and h_B we find by the formulas

$$h_B^{n+1} = h_B^n + \tau_n p^n \tag{3.18}$$

$$\varphi^{n+1}(x) = \varphi^n(x) + \tau_n[u_1^n(x) + p^n u_2^n(x)], \tag{3.19}$$

$$\psi^{n+1}(x) = \psi^n(x) + \tau_n[v_1^n(x) + p^n v_2^n(x)], \tag{3.20}$$

which are analogous to (2.5) and directly follow from the discretization of the differential equations (3.7). We calculate the iterational parameter τ_n by the formula of Ermakov-Kalitkin (2.7).

4. Discretization of the linearized problem

We solve numerically the obtained in the previous paragraph linear equations (3.9)–(3.17). For this aim we use the differential scheme based on the approximative presentation of the solution by cubic splines.

Let us consider a linear ordinary differential equation of second order with boundary conditions of Neuman.

$$-w'' + q(x)w = r(x),\ x \in (-\Delta, \Delta), \tag{4.1}$$

$$w'(\pm\Delta) = A. \tag{4.2}$$

We suppose that $r(x)$ and $q(x)$ are known functions of the independent variable x, and A is a given constant. At a suitable choice of the functions $r(x)$ and $q(x)$ and of the parameter A we achieve the linearized equations (3.9)–(3.16) of CAMN.

We introduce in the interval $[-\Delta, \Delta]$ an uniform grid

$$-\Delta = x_0, x_1, x_2, \ldots, x_N = \Delta$$

with a step $h = x_{i+1} - x_i,\ i = 0, 1, 2, \ldots, N-1$. We look for a solution of the equation (4.1) in the form of a cubic spline $S(x)$ of a class C^2 with knots coinciding with the knots of the introduced grid. Such a spline in the interval $[x_i, x_{i+1}]$ is defined by the formula [5]

$$S(x) = (1-s)w_i + sw_{i+1} - \frac{h^2}{6}s(1-s)[(2-s)M_i + (1-s)M_{i+1}]. \tag{4.3}$$

Here we have set $s = \frac{x-x_i}{h}$, and M_i are the second "moments" of the spline $M_i = S''(x_i)$. The conditions for the continuity of the first derivative of the spline at the interval points of the grid have the form

$$M_{i-1} + 4M_i + M_{i+1} = \frac{6}{h^2}(w_{i-1} - 2w_i + w_{i+1}). \tag{4.4}$$

According to the collocation method we require in the knots of the grid the following condition to be fulfilled

$$-S_i'' + q_i S_i = r_i, \tag{4.5}$$

where we have set $q_i = q(x_i),\ r_i = r(x_i)$.

After the elimination of the moments M_i from the conditions (4.4) with the help of (4.5) we reach the system of $N-1$ algebraic equations

$$aw_{i-1} + b_i w_i + c_i w_{i+1} = d_i, \tag{4.6}$$

with coefficients

$$a_i = -1 + \frac{h^2}{6}q_{i-1},\ b_i = 2 + \frac{2h^2}{3}q_i,\ c_i = -1 + \frac{h^2}{6}q_{i+1}, \tag{4.7}$$

and right side

$$d_i = \frac{h^2}{6}(r_{i-1} + 4r_i + r_{i+1}). \tag{4.8}$$

In order to receive a closed system accordingly to the form of the boundary conditions (4.2) for the equation (4.1) we use the two boundary conditions of first order [12] for the spline

$$2M_0 + M_1 = \frac{6}{h}\Big(\frac{w_1 - w_0}{h} - w_0'\Big), \quad M_{N-1} + 2M_N = \frac{6}{h}\Big(w_N' - \frac{w_N - w_{N-1}}{h}\Big).$$

If we eliminate the magnitudes $M_0,\ M_1,\ M_{N-1}$ and M_N from the last two equations with the help of the collocation conditions (4.5) we obtain the required two algebraic equations

$$b_0 w_0 + c_0 w_1 = d_0, \quad a_N w_{N-1} + b_N w_N = d_N. \tag{4.9}$$

Here the coefficients and the right sides are

$$b_0 = 2 + \frac{2h^2}{3}q_0,\ c_0 = -1 + \frac{h^2}{6}q_1, \tag{4.10}$$

$$a_N = -1 + \frac{h^2}{6} q_{N-1},\ b_N = -1 + \frac{h^2}{6} q_N, \tag{4.11}$$

$$d_0 = \frac{h^2}{6}(2r_0 + r_1) + hA,\ d_N = \frac{h^2}{6}(2r_N + r_{N-1}) - hA. \tag{4.12}$$

The equations (4.6) and (4.9) form a tri-diagonal system of $N + 1$ linear algebraic equation for the values of the spline interpolating the solution at the grid knots. It follows from the kind of coefficients $a_i,\ b_i$ and c_i that the matrix of this system has a diagonal domination. Therefore, to solve this system we can use the sweep method without a choice of a leading element.

The estimate of the error of the constructed approximate solution is considered in book [12].

5. Some numerical results and an investigation of the critical curves

Based on the above presented algorithm and the spline-differential scheme a program in the language FORTRAN for the calculation of the bifurcation curves of the solutions of the boundary problems (1.1)–(1.4) is composed. The basic input parameters of the program are:

Δ – half-length of the junction;

μ – width of the non-homogeneity;

h_B – voltage of the magnetic field at the ends of the junction;

γ – current

Three regimes of work are provided:

i. regime of looking for solutions at known initial approximation;

ii. regime of variation of a given solution with respect to the parameter h_B (or γ);

iii. regime of variation of a given solution with respect to the width μ of non-homogeneity.

In the last two cases as an initial approximation for the current value of the varied parameter the received for the previous value of this parameter solution is chosen. This guarantees a fast convergence (usually, no more than 2-4 iterations are sufficient).

At the variation of initial approximations the algorithm can be convergent to one and the same solution. Analogously to [15] in order to avoid the repetition, before the calculation of the physical characteristics it is necessary to verify the identity of the newly obtained solution with the solutions received earlier.

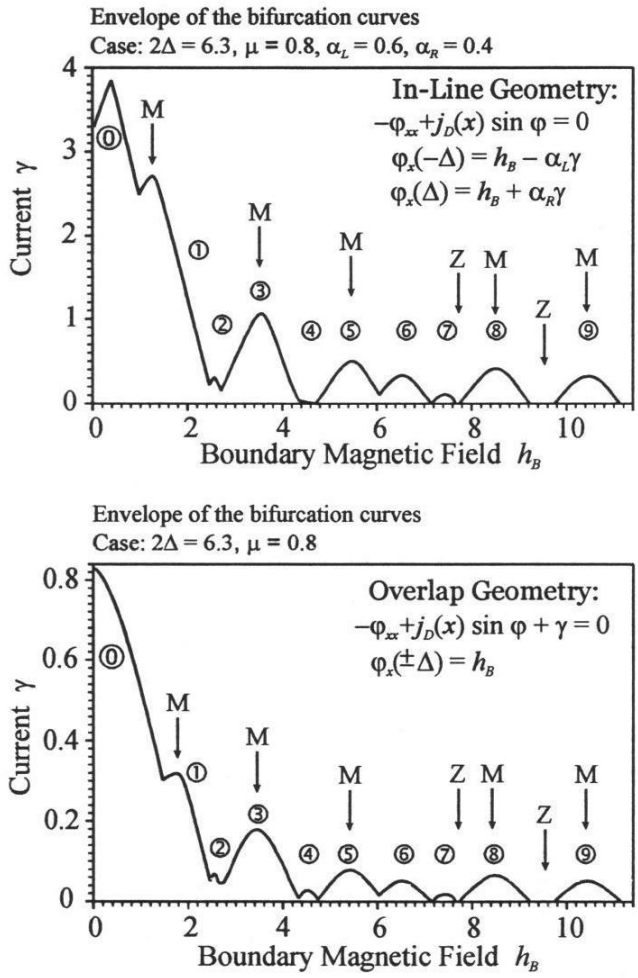

Fig. 3

It is important also to note that at an "arbitrary" initial approximation the presented above algorithm does not always converge to the stable solution corresponding to $\lambda = \lambda_{\min}$. The fixed value of the parameter λ coincides with some of higher EV of SLP. In mathematical point of view, however, we have a bifurcation of an unstable solution into unstable one. This phenomenon is

physically nonobservable. That is why if it is necessary the program provides a verification of the number of zeros of every received solution accordingly to the theorem for the oscillations [18].

In fig. 3 there are presented the received at the numerical experiments parts of a typical envelope of bifurcation curves (critical curves) of the kind "current-magnetic field", corresponding to the stated in the introduction two geometries of JJ. The values of the parameters are given as follows: length of JJ $2\Delta = 6.3$, width of non-homogeneity $\mu = 0.8$ and a parameter $\alpha_L = 0.6$ ($\alpha_R = 0.4$). The comparison with the data received by Vystavkin et al [7] and Larsen et al [6] (see fig.2) shows a good qualitative coincidence between the numerical and the experimental results, the more so, as the indicated data is related to patterns of JJs with different geometrical and physical characteristics. It should be pointed out that the presence in the constructed by a numerical way critical curves and the three mentioned above experimental effects:

$\succ$ a shift of the absolute maximum from the zero boundary magnetic field;

$\succ$ the presence of local maximums (marked by the letter "M") disturbing the Fraunhopher lattice [1];

$\succ$ the presence of "damping zones" of the current at big values of h_B (marked by a letter "Z").

The last two effects are obtained in [6] in experiments with JJ the dielectric layer of which is a "lattice" f resistive non-homogeneity.

In our opinion, a quantitative coincidence between numerical and experimental data can be reached. First, by relating the data to the same pattern of JJ, and also, by making more precise the physic-mathematical model (for example taking into account the inductance of JJ [23]).

Let us consider more precisely the structure of the critical curves in view of the carried out numerical experiment.

The concrete envelopes (critical curves) corresponding to fixed values of the parameters of JJ consist of separate parts (bifurcation curves) each of which is numbered and corresponds to a concrete solution of the problem (1.1), (1.2) or (1.1), (1.4).

In table 1 the basic data for these solutions at the value $\gamma = 0$ of the current are presented. The following notations are used:

$$\Delta\varphi = \varphi(\Delta) - \varphi(-\Delta) \tag{5.1}$$

- full magnetic flux for the solution;

Parameters of the bifurcation solutions
in onedimensional junction with one nonhomogeneity

$2\Delta = 6.3, \quad \mu = 0.8, \quad \gamma = 0$

	h_B	$\Delta\varphi/2\pi$	A	E	FE	φ_L	φ_R	q_{avr}
$S0$	2.0236	0.9776	2.0	1.168	21.767	3.2120	9.3543	0.2503
$S1$	-1.0444	0.4371	1.0	0.9963	5.1023	1.7685	4.5147	0.0413
$S1$	2.5758	2.1003	3.0	2.429	53.421	2.8266	16.0229	0.1827
$S2$	2.2852	2.2426	3.364	2.706	53.848	4.1527	18.2438	0.1972
$S2$	2.7843	2.1003	3.4252	3.547	75.4301	5.5180	22.4183	0.1329
$S2$	2.2852	2.2426	2.636	2.706	53.848	0.6058	14.6967	0.1972
$S2$	2.7843	2.1003	4.5748	3.547	75.4301	2.7145	19.6148	0.1329
$S3$	2.5419	2.8297	3.0	3.818	75.736	0.5349	18.3147	0.1006
$S3$	4.3789	4.1451	5.0	7.402	173.2635	2.6858	28.7301	0.0589
$S4$	4.774	4.7083	5.624	9.359	216.111	3.0766	32.6594	0.0396
$S4$	4.281	4.3026	4.516	7.935	179.205	0.3536	27.3874	0.0570
$S5$	4.703	4.8761	5.0	9.982	223.949	0.3894	31.0265	0.0365
$S6$	5.883	6.0811	8.0	15.152	346.004	6.0283	44.2372	0.0229
$S7$	7.652	7.6093	9.0	23.343	552.574	4.3691	52.1796	0.0245
$S8$	7.738	7.8878	8.0	25.033	583.753	0.3525	49.9130	0.0193
$S9$	9.747	9.8597	10.0	38.738	913.719	0.4407	62.3911	0.0173

Table 1

$$A(h_B, \gamma) = \frac{1}{4\pi\Delta} \int_{-\Delta}^{\Delta} \varphi(x, h_B, \gamma) dx \tag{5.2}$$

- dimensionless "area" of the figure, surrounded by the graph of the solution $\varphi(x)$ in the interval $[-\Delta, \Delta]$;

$$E = \int_{-\Delta}^{\Delta} \Big[\frac{\varphi_x^2}{2} + j_D(x)(1 - \cos\varphi) + \gamma\varphi \Big] dx \tag{5.3}$$

- energy;

$$FE = E + h_B \Delta\varphi \tag{5.4}$$

- full energy for the concrete solution.

The section with number 1 corresponds to the so called Meissners ("vacuum") solution which at a current $\gamma = 0$ and a boundary magnetic field $h_B = 0$ (i.e. far from the bifurcation values of the physical parameters is the trivial solution

$$\varphi_k(x) = k\pi, \;\; k = 0, \pm 1, \pm 2, \ldots$$

At $k = 0, \pm 2, \pm 4, \ldots$ for the sake of equality $|q(x)| = j_D(x)$ Meissners solutions are stable, and at odd values of k – unstable.

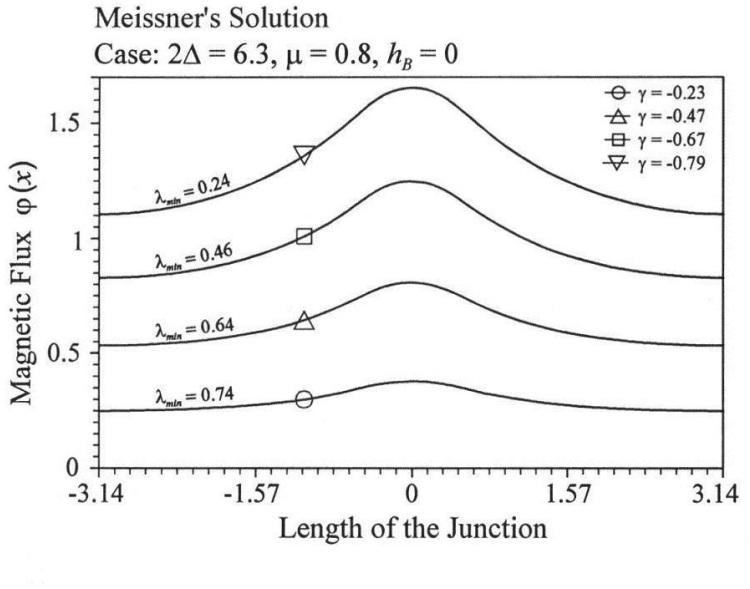

Fig. 4

The character of the deformation of Meissners solution at non-zero values of the current γ is shown in fig 4. It is seen that at an increase of $|\gamma|$ the magnetic flux $\varphi(x)$ in JJ as well as the magnetic field (the derivative $\varphi_x(x)$) concentrate themselves in the neighbourhood of the non-homogeneity, moreover, the corresponding minimal EV $\lambda_{\min}$ decreases coming nearer the bifurcation value $\lambda_{\min} = 0$.

The deformation of Meissners solution at a change of the external magnetic field h_B (see fig. 5) in contrast to the previous case consists of a concentration of the magnetic field $\varphi_x(x)$ at the ends of JJ.

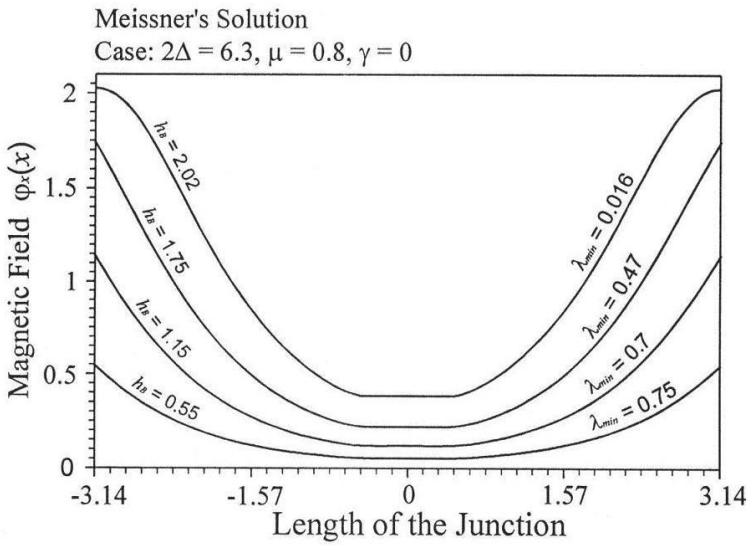
Meissner's Solution
Case: 2Δ = 6.3, μ = 0.8, γ = 0
Magnetic Field φx(x)
Length of the Junction
hB = 2.02
hB = 1.75
hB = 1.15
hB = 0.55
λmin = 0.016
λmin = 0.47
λmin = 0.7
λmin = 0.75
2
1.5
1
0.5
0
-3.14
-1.57
0
1.57
3.14

Fig. 5

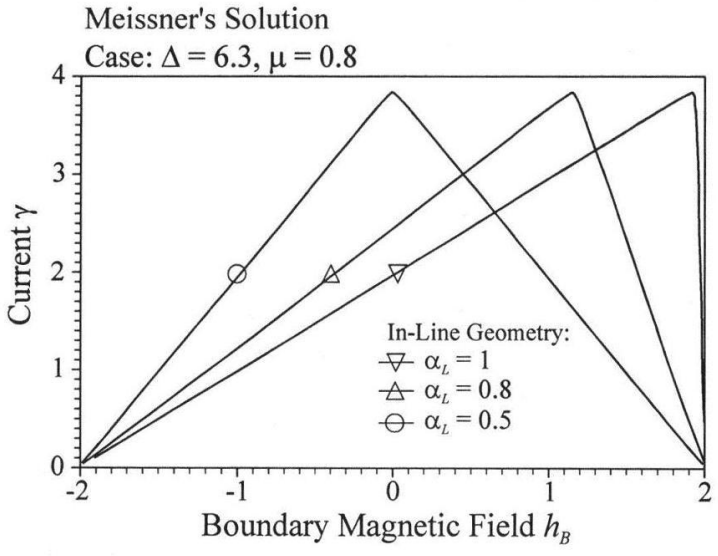
Meissner's Solution
Case: Δ = 6.3, μ = 0.8
Current γ
Boundary Magnetic Field hB
In-Line Geometry:
αL = 1
αL = 0.8
αL = 0.5
4
3
2
1
0
-2
-1
0
1
2

Fig. 6

The asymmetry of boundary conditions (the possible injection of a current through the ends of JJ) exerts a considerable influence on the form of bifurcating curves for the Meissners solution. This basic numerical fact is illustrated in details in fig.6 for several values of the normalizing parameter α_L and consists of a shifting at $\alpha_L \neq 0.5$ ("antisymmetric" boundary conditions) of the maximums of the bifurcation curves from the point $h_B = 0$. The magnitude of such a shifting depends essentially on the size of the parameter α_L. Conversely, in the "symmetric" case of JJ, described by the boundary problem (1.1) and (1.2), the maximums of the bifurcation curves (compared with fig.1) for Meissners solution are always at $h_B = 0$ (see [4,15]).

The section of the critical curve, marked with $\leftarrow$, corresponds to the solution which for an infinite homogeneous JJ or a non-homogeneous JJ with a single Dirac's non-homogeneity, has an analytical form.

$$\varphi(x) = 4 \operatorname{arctg} \exp\{\pm x\}, \tag{5.5}$$

with full energy $F = 8$. The sign + in the above equation corresponds to a distribution of the magnetic flux along the length of JJ, which in the physical literature is called basic "fluxon" and its derivative $\varphi_x(x)$ — "soliton". The full magnetic flux of the basic fluxon is $\Delta\varphi = 2\pi$. The solution (5.5) with a sign "$-$" is known as "antifluxon" with a derivative, called "antisoliton" and the corresponding magnetic flux is $\Delta\varphi = -2\pi$, respectively.

At a current $\gamma = 0$ the maximum (the minimum of the basic soliton) of the antisoliton of the magnetic field is in the center of non-homogeneity $x = 0$. At $\gamma \neq 0$ the extremum of the soliton displaces itself [24] depending on the sign of γ to the left or to the right from the point $x = 0$, as a result the problem has 4 solutions of the indicated form - "left" or "right" solitons (below we use the notations S_L and S_R, respectively) and antisolitons (A_L and A_R). In mathematical point of view the existence of these solutions is a consequence of the properties of the symmetry of the considered problem (see for example [23]).

In fig. 7 the diagram of the dependence $\lambda_{\min}(\gamma)$ of the solution of JJ in overlap geometry (the problem (1.1), (1.2)) at $2\Delta = 6.3$ and zero magnetic field h_B is shown. The points B_1 and B_4 are points of a bifurcation of Meissners solution, and B_2 and B_3 – solutions of the basic fluxon. The bifurcational diagram for any solution is a geometric lock of the indicated form.

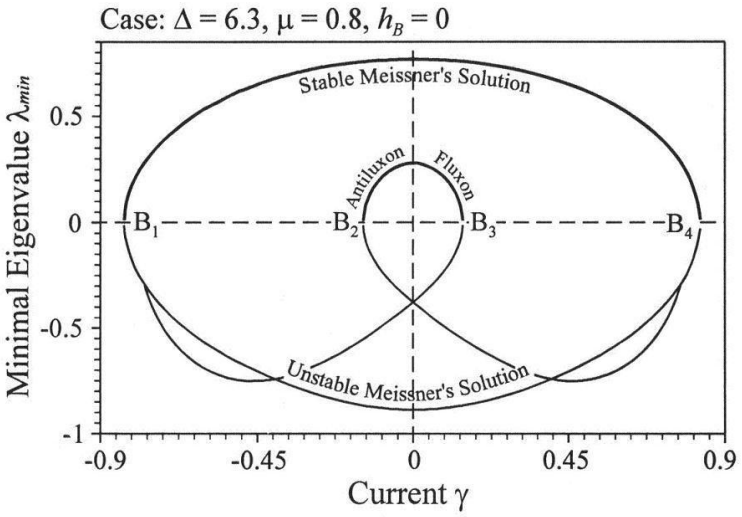

Fig. 7

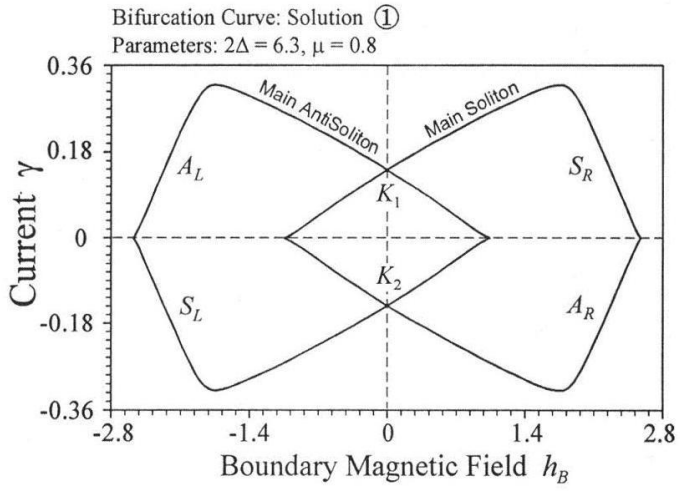

Fig. 8

Especially, in fig. 8 the full bifurcation diagram for the basic fluxon S_1 is shown. As it is seen, the corresponding curves for the solutions S_R and A_L,

and also for S_L and A_R intersect in the points K_1 and K_2, forming fluxon-antifluxon "crosses". This fact is received for the first time numerically in the work [4] and it is confirmed experimentally in the paper [7].

Reducing the width μ of the non-homogeneities the fluxon and antifluxon sections of the diagram are displaced to the right (to the left) along the axis h_B and at sufficiently small μ "the crosses" can disappear from the upper half-plane $\lambda_{\min} \geq 0$, transfering upon the unstable solutions.

At further increasing of the external magnetic field h_B (see fig.3) in JJ new solutions are "generated", the most typical of which are presented in fig.9 and fig.10 (the numbering corresponds to that of fig.3).

First of all, we shall note that every solution $\varphi(x)$ has its own region of stability at the change of the current γ and the boundary magnetic field h_B in which the solution exists.

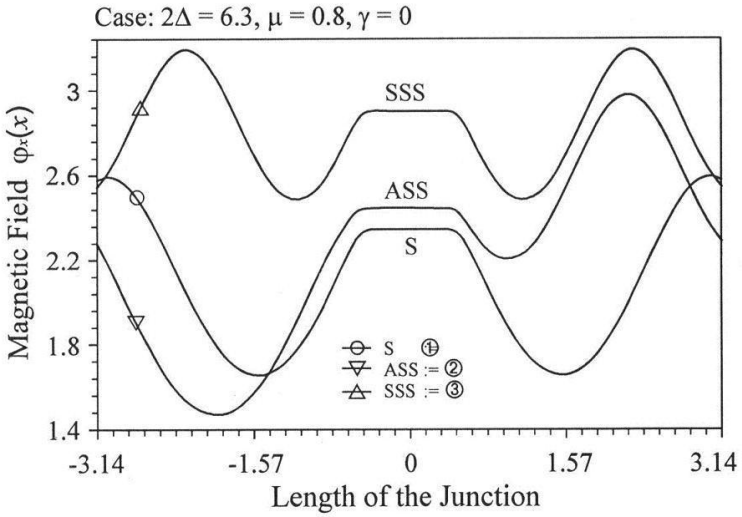

Fig. 9

The magnetic fields, corresponding to the marked by $\uparrow$ and $\rightarrow$ solutions can be considered as such non-linear deformations of the basic soliton, at which from the left and from the right of the junction either one soliton (antisoliton) (see the curve SSS in fig.9 corresponding to the solution $\rightarrow$) or a soliton - antisoliton couple (see the curve ASS of fig.9 corresponding to the solution $\uparrow$) is added. The symmetric solution SSA is not shown. The solution ASA exists in the symmetric with respect to the axis γ interval of the axis h_B.

This chain process can be visualized by the following scheme.

$$
S \Rightarrow \begin{cases}
S \oplus S \oplus S \equiv SSS \Rightarrow \begin{cases} S \oplus SSS \oplus S \equiv SSSSS \\ A \oplus SSS \oplus S \equiv ASSSS \\ S \oplus SSS \oplus A \equiv SSSSA \end{cases} \\
A \oplus S \oplus S \equiv ASS \Rightarrow \begin{cases} S \oplus ASS \oplus S \equiv SASSS \\ A \oplus ASS \oplus S \equiv AASSS \\ S \oplus ASS \oplus A \equiv SASSA \end{cases} \\
S \oplus S \oplus A \equiv SSA \Rightarrow \begin{cases} S \oplus SSA \oplus S \equiv SSSAS \\ A \oplus SSA \oplus S \equiv ASSAS \\ S \oplus SSA \oplus A \equiv SSSAA \end{cases}
\end{cases}
$$

(We use formally the symbol $\oplus$ to denote the (non-linear) process of the change of the solution. Graphically $\oplus$ expresses "addition" or "subtraction" of "vortexes" (solitons) to the graph of the derivative)

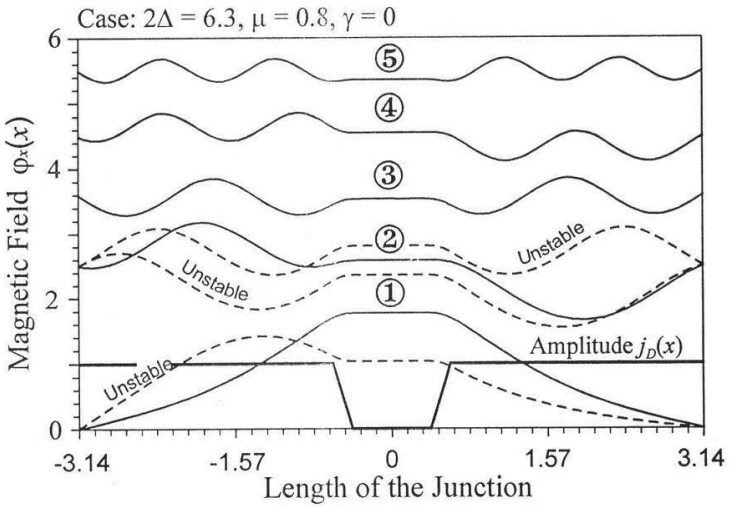

Fig. 10

The "addition" of a single soliton or antisoliton to one side of the non-homogeneity leads to unstable solution. Such unstable solutions are shown in fig.10 by dotted lines.

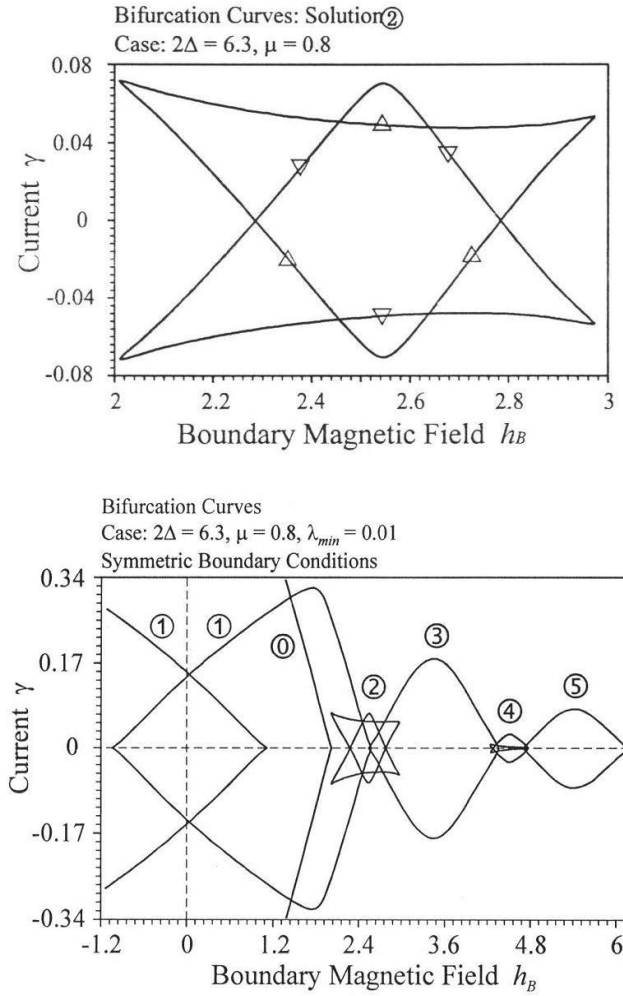

Fig. 11

The bifurcation dependences (see fig.11) for the four solutions of the kind ↑

$$S \Rightarrow \begin{cases} SSA \\ ASS \end{cases},$$

exist by couples, corresponding to "the left" and "the right" solitons (the posi-

tive and negative values of the external current γ). The symmetric with respect to the ordinate axis dependences

$$A \Rightarrow \begin{cases} SAA \\ AAS \end{cases}$$

exist at negative h_B. In fig.11 by the symbol "∇" is marked the curve representing the solution SSA_R and by the symbol Δ – the solution ASS_L.

According to what has been said it follows that the presence of the local extremums in the critical curves is a consequence of the different "level of stability" of the "pure" soliton and mixed solution-antisoliton solutions.

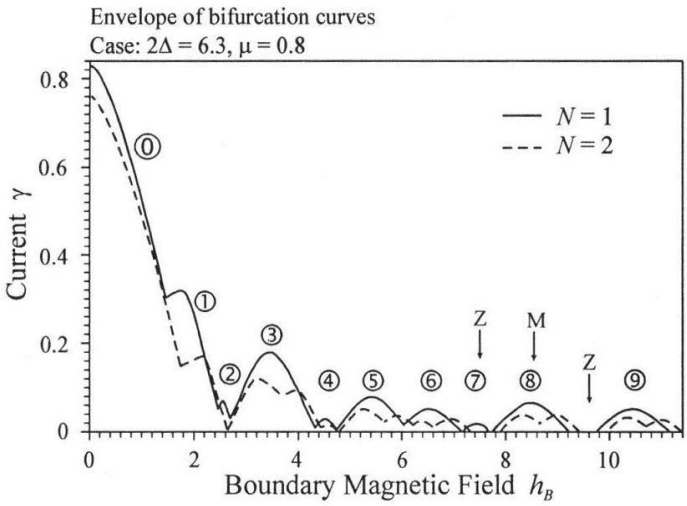

Fig. 12

Finally, in fig.12 the critical curves for JJ with one ($N = 1$) and two ($N = 2$) identical non-homogeneities are shown. It is seen that the basic differences consist of non-coincidence of the amplitudes and the localization of the local extremums and of the generation of new ones at ($N = 2$), and of non-coincidence of the damping zones, too. Hence, it follows that we must accept as a basic factor for the peculiarities of the critical curves in JJ the presence of non-homogeneity in the dielectric layer.

In this way, the disturbing of the Fraunhopher chain [1] in the critical dependence of the kind "current-magnetic field" for non-homogeneous JJ (the presence of the local extremums and damping zones of the current γ) is inherent

to the JJ with a single non-homogeneity and at big values practically does not depend on the kind of boundary conditions.

References

[1] A. Bapone, J. Paterno. Effect of Josephson, M. "Mir", 1984. (in Russian)

[2] Yu.S. Galpern and A.T. Filippov, Sov. Phys. JETP, 86 (1984), p. 1527.

[3] B. Josephson, Possible new effect in superconductive tunneling, Phys. Lett., v. 1, No 7, 1962, p.251.

[4] A.T. Filippov, Yu.S. Galpern, T.L. Boyadjiev and I.V. Puzynin. Critical currents in Josephson junctions with microhomogeneities attracting solitons, Phys. Lett. A, 1987, v. 120, No 1.

[5] B.A. Malomed, A.V. Ustinov, Pinning chain of Josephson vorteses in periodical junctions: theory and experiment, J. of Low Temp. Phys. Vol. 15, 1989, p. 1128–1137.

[6] B.H. Larsen, J. Mygind, A.V. Ustinov, Commensurate fluxon states in long Josephson Junctions with inhomogeneities. Physica B, v. 194–196 (1994), pp. 1729–1730.

[7] A.N. Vystavkin, Yu.F. Drachevskii, V.P. Koshelets and I.L. Serpuchenko. Detection of Statistically Coupled States of Fluxons in Disturbed Josephson Junctions with an inhomogeneity, J. of Low Temp. Phys., v.14, 646 (1988).

[8] M.K. Gavurin, Non-linear functional equation and continuous analogues of iteration methods. Izv. VUZ, Mathematics, v.5(6), 18–31 (1963). (in Russian)

[9] I.V. Puzynin, I.V. Amirkhanov, E.V. Zemlyanaya, V.N. Pervushin, T.P. Puzynina, T.A. Strizh and V.D. Lakhno, in "Physics of Elementary Particles and Atomic Nuclei", JINR Dubna, 1999, vol.30, No 1, p.210. (in Russian)

[10] B. Sendov, V. Popov, Numerical methods "Nauka", Sofia, 1982. (in Bulgarian)

[11] V.V. Ermanov and N.N Kalitkin, Optimal step and regularization of Newtons method, USSR Comp. Math. and Math. Phys., v.21(2), p. 235 (1981).

[12] Yu.S. Zavialov et al., Methods of spline - functions. M., GRFML, 1980. (in Russian)

[13] N.V. Alexeeva, Numerical investigation of periodical soliton-like solutions in Josephson lattices, Diplom FMI - Sofia, 1996. (in Bulgarian)

[14] J.G. Caputo, N. Flytzanis, Y. Gaididei, N. Stefanakis and E. Vavalis, Stability analysis of static solutions in a Josephson junction, Superconducting Science and Technology, 13(2000), pp. 423–438.

[15] T.L. Boyagjiev, D.V. Pavlov and I.V. Puzynin, Newtons algorithm for calculation of critical parameters in one-dimensional inhomogneous Josephson junctions, Comm. of JINR, P11–88–409, Dubna, 1988. (in Russian)

[16] N.V. Alexeeva and T.L Boyadjiev, Periodic bound states in Josephson lattices of resistive inhomogeneities, Bulg. J. of Physics, No 1, 2, 1977.

[17] T.L Boyadjiev and M.D. Todorov, Numerical Investigation of a bifurcation problem with free boundaries arising from the Physics of Josephson Junctions, Mathematical Modeling, v. 12, No 4, 2000, p. 61. (in Russian)

[18] B.M. Levitan, I.S. Sargsjan, Introduction to spectral Theory, Transl. Math. Monographs, AMS, Providence, RI, 1975.

[19] Yu.S. Galpern and A.T. Filippov, Solid State Comm., v.48 (1983), p. 665.

[20] I.L. Serpuchenko, A.V. Ustinov, Solid State Comm., 68,7, 1988, p. 693.

[21] R. Fehrenbacher, V.B. Geshkenbein, G. Blatter, Pinning phenomena and critical currents in disordered long Josephoson junctions, Phys. Rev. B, v. 45, No 10 (1992), pp. 5450–5467.

[22] A.T. Filippov, T.L. Boyadjiev et al., Localization of solitons on small inhomogeneities in Josephson junctions, Preprint JINR, E17–89–106.

[23] T. Boyadjiev, S. Dimova, Modeling of bound states in long Josephson junctions, Mathematical modeling, v.9, No 5, 1977, p.37. (in Russian)

[24] D.W. McLaughlin, A.C. Scott, in "Solitons in action", Editors K. Longren and A. Scott, Academic Press, 1978.

P. Kh. Atanasova
Faculty of Mathematics and Informatics
University of Plovdiv
236 Bulgaria Blvd.,
4003 Plovdiv, BULGARIA
e-mail: poli@jinr.ru

Received 06 January 2005

T. L. Bojadjiev
Faculty of Mathematics and Informatics
University of Sofia
5 James Bourchier Blvd.,
1164 Sofia, BULGARIA
e-mail: todorlb@fmi.uni-sofia.bg

ЧИСЛЕНО МОДЕЛИРАНЕ НА ДЪЛГИ НЕХОМОГЕННИ ДЖОЗЕФСОНОВИ ПРЕХОДИ

П. Хр. Атанасова, Т. Л. Бояджиев

Резюме. В работата е представено числено моделиране на дълги нехомогенни джозефсонови преходи. Разгледани са преходи с "overlap" и "in-line" геометрия. Въпросът се свежда до нелинейна гранична диференциална задача от втори ред, която се решава числено. Изчисляването на бифуркационните точки е направено с прилагане на непрекъснатия аналог на метода на Нютон. Числените резултати се интерпретират и е показано добро съвпадение с експериментални данни. Работата е илюстрирана графично достатъчно пълно.